Contrast Enhancement and Background Suppression of Chemosensor Array Patterns with the KIII Model

Agustin Gutierrez-Galvez,[†] Ricardo Gutierrez-Osuna[*]
*Department of Computer Science, Texas A&M University,
College Station, TX 77843, USA*

Inspired by the ability of the olfactory bulb to enhance the contrast between odor representations, we propose a new hebbian learning rule that is able to increase the separability of odor patterns from gas sensor arrays. The proposed learning rule employs a hebbian term to build associations within odors and an anti-hebbian term to reduce correlated activity across odors. In addition to increasing the separability of patterns, the new learning rule can also achieve odor background suppression when combined with a habituation term. These two functions are demonstrated on Freeman's KIII, a neurodynamics model of the olfactory system. The system is first characterized on synthetic data, and also validated on experimental data from an array of chemical sensors exposed to organic solvents. © 2006 Wiley Periodicals, Inc.

1. INTRODUCTION

The olfactory bulb plays an important role in the processing of odorant information. It receives direct inputs from olfactory receptor neurons in the epithelium and reshapes this information through excitatory-inhibitory circuits, increasing the contrast across odor representations.[1] Borrowing inspiration from this computational function, this work proposes a learning rule to improve the discrimination of patterns from gas sensor array systems. The rule employs a hebbian term to correlate channels (e.g., features or sensors) that are active *within* an odor pattern, and an anti-hebbian term to decorrelate channels that are active *between* multiple odor patterns.

The proposed learning rule is validated on the KIII, a neurodynamics model of the olfactory system developed by Freeman and colleagues over the last 30 years.[2–5] With a few exceptions, the KIII model has gone largely unnoticed in the machine olfaction literature. Otto has applied the KIII to process data from FTIR

and chemical sensors[6–8] using habituation and hebbian learning. Our own prior work on the KIII model[9] has investigated the use of local habituation to depress the activity of channels that receive sustained input, allowing the model to segment odors into their individual components. In that case, however, the KIII relied on a statistical preprocessing stage to orthogonalize sensor patterns. In the present article, the preprocessing stage is replaced by the proposed contrast-enhancement learning rule in order to reduce the overlap between odor patterns, thus allowing the KIII to segment mixtures directly from raw sensor array patterns.

The article is organized as follows. Section 2 presents an overview of the electronic nose technology, the domain problem that our research is specifically addressing. The KIII model, along with specifics on our implementation, is reviewed in Section 3. Section 4 introduces the new hebbian/anti-hebbian learning rule for contrast enhancement. Section 5 describes a mechanism for mixture segmentation that combines the proposed learning rule with a local habituation term. In Section 6, the model is validated on experimental data from a gas sensor array. The article concludes with a discussion of our results.

2.   THE ELECTRONIC NOSE TECHNOLOGY

An electronic nose (e-nose) consists of an array of cross-selective gas sensors coupled with a pattern recognition engine capable of detecting, identifying, and quantifying volatile compounds.[10] E-noses represent a low-cost and high-throughout alternative to odor measurement, traditionally performed with analytical instruments or human panels. Several types of gas sensors are commonly employed in e-noses, including metal oxide semiconductors (MOS), quartz crystal microbalance (QCM), surface acoustic wave (SAW), and organic conducting polymers (CP).[11] Among these, MOS sensors are particularly attractive for our research because of their high sensitivity, the relatively simple instrumentation required, and the ability to modulate their selectivity.[12] MOS sensors are chemoresistors: When exposed to a volatile compound the conductivity of the sensing layer changes as a result of chemical reactions with gaseous molecules at the surface of the sensor. These reactions are dependent on temperature, and, as a result, the selectivity of MOS materials can be controlled by selecting an appropriate operating temperature at the surface of the material. This property is of particular interest for our research because it allows us to generate a large amount of information by modulating the temperature of the device while it is exposed to different volatile chemicals.

Pattern recognition for e-noses has been traditionally performed with statistical methods and artificial neural networks.[13] Among the statistical methods, the most commonly used are principal components analysis, linear discriminant analysis, and various forms of multilinear regression (e.g., partial least squares). Among the artificial neural network models, multilayer perceptrons, radial basis functions, and self-organizing maps are most commonly used. Despite the parallelisms between broadly tuned sensor arrays and the olfactory system, biologically inspired processing approaches have been largely disregarded in the machine olfaction

community. For a thorough overview of these models, the reader is referred to Refs. 14 and 15.

3. THE KIII MODEL

The KIII is an oscillatory neural network modeled after the basic architecture of the olfactory system. As shown in Figure 1a, the KIII contains building blocks for the three main stages in the olfactory pathway: epithelium, bulb, and cortex.[2] The KIII is a hierarchical model of simple processing units. The basic unit is the K0, which represents a neuron population.[5] All higher level structures in the KIII are made of interconnected K0 sets. Two K0 sets with the same sign (i.e., either excitatory or inhibitory) can be laterally connected to form a KI set. Similarly, two KI sets of different signs can be connected to form a KII set. KII sets are the most critical processing blocks, as they are responsible for the oscillatory behavior of the model. K0 sets have fixed coupling coefficients, which have been painstakingly obtained from experimental neurobiological data by Freeman and colleagues.[5] The last hierarchical level is the KIII model itself, which consists of three stages of coupled KII sets with feed-forward and feedback connections.
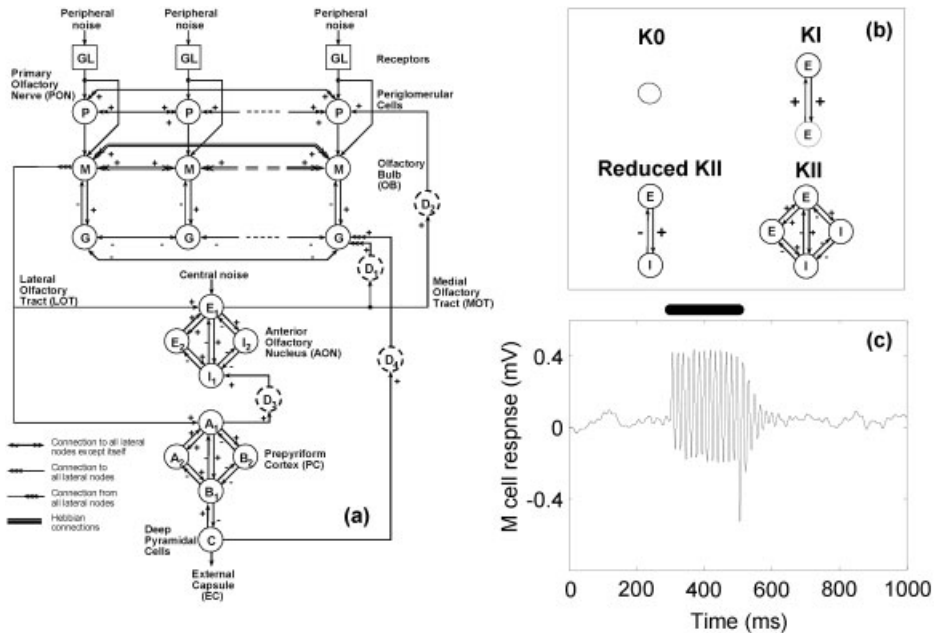

Figure 1. (a) Architecture of the KIII model. Hebbian learning is performed by adapting mitral-to-mitral connections (double lines in the figure). (b) The k sets: K0, KI, and KII. (c) Activity of a mitral cell (M). The M cell is in a basal state until a stimulus is presented (300 ms to 500 ms). Once the stimulus is removed, the M cell returns to the basal state.

The dynamics of a K0 set are modeled with a second-order nonlinear differential equation, with a forcing term for incoming connections from other K0 sets. As a result of its hierarchical structure with widespread lateral, forward, and recurrent connections, the KIII model is described by a system of massively coupled second-order nonlinear differential equations. This complex system gives rise to a locally stable but globally unstable behavior in a very high-dimensional space. In the absence of external input, the system remains in a chaotic basal state, consistent with those observed in the olfactory system through electroencephalogram (EEG) recordings.[2] When an input is presented, the KIII jumps into a limit cycle attractor that is specific to the input stimulus. Once the stimulus is removed, the KIII returns to its basal state. This type of information coding into oscillatory patterns (i.e., limit cycle) has been shown to improve the system's capacity and noise immunity.[3,16,17]

Odor stimuli are presented to the KIII as activation patterns across an input layer of receptors. Each receptor is connected to a KII set through a periglomerular cell, forming a channel. Learning a new odor in the KIII leads to the creation of a new limit-cycle attractor to which the system will converge when a similar odor is presented. This is achieved by means of hebbian learning at the level of mitral to mitral connections (double lines in Figure 1). This form of learning allows the KIII to recover not only the originally stored pattern when presented at the input, but also incomplete or distorted versions of it. Therefore, the KIII acts as an associative memory. The global behavior of the KIII is scale invariant (i.e., independent of the number of input channels), an essential property to allow the model to process sensor-array patterns of any input dimensionality. The output of the KIII model is normally "read out" at the bank of KII sets in the olfactory bulb.[18] Specifically, in this article we consider the AC amplitude of oscillations in mitral cells as the output of the model.

We employ a KIII model with reduced KII sets (Figure 1a). Model parameters were selected from Ref. 4 and fine-tuned to ensure (i) an aperiodic basal state with $1/f$ power spectra, (ii) a limit-cycle behavior when an input is introduced, and (iii) a return to the aperiodic basal state when the input is removed. Final model parameters are summarized in Table I. The KIII model was implemented in MATLAB, using fourth-order Runge-Kutta ODE integration with a time step of 1.0 ms. Initial conditions for all variables and their derivatives were set to zero.

Table I.   Parameters of the KIII model.

q^P	1.824	w_{EI}	1.426	w_{MIP}	0.5	w_{G1D4}	2.305
w_{PPL}	0.9	w_{IE}	1.372	w_{E1M1}	1.311	**Ts1**	20
k_{PR}	0.35	w_{II}	1.571	w_{A1M1}	1.717	**Te1**	11
q^{OB}	5	q^{PC}	5	w_{GGL}	0.1	**Ts2**	22
w_{MG}	1	w_{AA}	0.823	w_{CB1}	1.543	**Te2**	15
w_{GM}	2.6	w_{AB}	1.938	w_{B1C}	0.698	**Ts3**	21
k_{M1R}	1	w_{BA}	1.947	w_{G1D1}	2.305	**Te3**	12
q^{AON}	5	w_{BB}	2.354	w_{PD2}	1.087	**Ts4**	30
w_{EE}	1.202	q^C	5	w_{I1D3}	2.553	**Te4**	24

4. CONTRAST ENHANCEMENT THROUGH HEBBIAN/ANTI-HEBBIAN LEARNING

Following Yokoi et al.,[19] contrast enhancement in the olfactory bulb results from inhibition of mitral cells by nearby granule interneurons. This inhibition has the effect of reducing the molecular tuning range (i.e., increasing specificity) of a mitral cell relative to that of the olfactory receptor neurons that converge onto it, effectively orthogonalizing patterns across odors. This computational function can be achieved by means of anti-hebbian learning,[20] which leads to a decorrelation of the inputs to the system. The anti-hebbian learning rule is the opposite of the hebbian rule and states that the strength of the connection between two neurons should decrease when both activate simultaneously:

$$\Delta w_{kl} = -x_k x_l \tag{1}$$

where x_k and x_l are the kth and lth inputs to the system.

Application of the anti-hebbian rule to the KIII model is not trivial because of the oscillatory nature of the KII sets: The interaction between laterally connected oscillators is a vector operation. Depending on the relative phase of the two oscillators, it is therefore possible for an inhibitory connection to have an excitatory effect. To address this problem, we propose a new learning rule that avoids negative connections by combining hebbian and anti-hebbian terms. The role of the hebbian term is twofold. First, it preserves the associative-memory function of the KIII, allowing the model to learn odor-specific attractors. Second, it provides positive mitral-to-mitral connections, which are subsequently reduced by an anti-hebbian term without the risk of becoming negative.

Assume an M-dimensional pattern recognition problem with N odor patterns $p^i = [x_1^i x_2^i \ldots x_M^i]^T$; $1 \leq i \leq N$. The lateral connectivity matrix between mitral cells is computed with the following outer-product rule:

$$\beta = \overbrace{\sum_{i=1}^{N} p^i \cdot (p^i)^T}^{\text{hebbian}} - \overbrace{\sum_{i=1}^{N} \sum_{\substack{j=1 \\ j \neq i}}^{N} p^i \cdot (p^j)^T}^{\text{anti-hebbian}} \tag{2}$$

The first term in Equation 2 is the hebbian rule, which strengthens the connection between neurons that are active *within* a pattern. The second term is the anti-hebbian component, which reduces the connection weights between neurons that are active for multiple patterns, on the average reducing the overlap *across* patterns. Negative mitral-to-mitral connections are avoided by forcing to zero all elements in Equation 2 that become negative.

4.1. Formal Analysis

To isolate computational function from nonlinear dynamics intricacies of the KIII model, a formal analysis of the proposed learning rule is performed on a simplified feed-forward network with linear neurons. This simplified model is
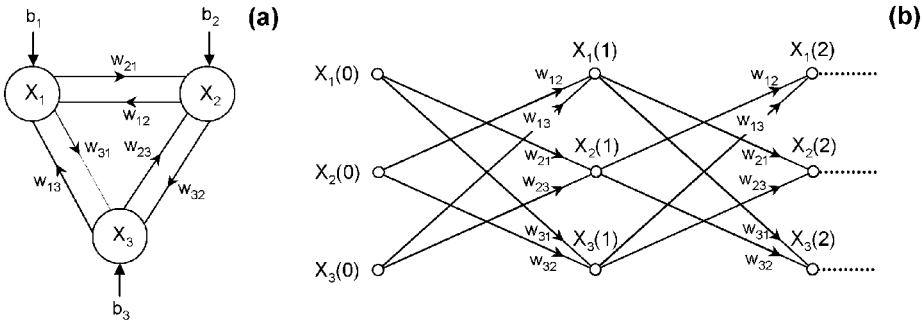
Figure 2. Unfolding in time of a recurrent network. (a) Fully laterally connected neural network. (b) Signal-flow graph of the recurrent network unfolded in time.

equivalent to the unfolding in time of a recurrent structure with linear neurons (Ref. 21, pp. 732–789). Figure 2b shows the unfolding of the fully laterally connected network in Figure 2a. At any specific time t, the activity on the network $x_i(t)$ is computed as:

$$x_i(t) = w \cdot x_i(t-1) + b_i \tag{3}$$

The evolution of this system will differ from that of the KIII because of the nonlinear behavior of the K0 sets. However, the effect of one single linear step will be similar in both systems, and much information about the effect of the learning rule on the recurrent network can still be gained by studying this simplified model.

In this study, the bias term will be assumed to be zero; this will allow us to isolate the effect of learning on the output of the system. Specifically, we consider a network with M fully connected neurons, analogous to the interconnectivity between mitral cells in the KIII model. This network is the main responsible for the processing of information in the model. We also assume that N nonnegative patterns $p^i = [x_1^i x_2^i \ldots x_M^i]^T$; $1 \leq i \leq N$; $x_j^i \geq 0$ have been stored according to Equation 2. When presented with one of these previously stored patterns p^k, the output of a single linear step becomes

$$w \cdot p^k = \sum_{i=1}^{N} p^i \cdot (p^i)^T \cdot p^k - \sum_{i=1}^{N} \sum_{\substack{j=1 \\ j \neq i}}^{N} p^i \cdot (p^j)^T \cdot p^k \tag{4}$$

Because the projection matrix w consists of the outer product of training patterns p^i, this linear transformation projects the M-dimensional input space onto the N-dimensional space spanned by the training patterns p^i. Therefore, the output of the system can be expressed as a linear combination of the stored patterns $\{p^i\}$. Separating the terms containing the input pattern p^k from the rest:

$$w \cdot p^k = p^k \cdot (p^k)^T \cdot p^k + \sum_{\substack{i=1 \\ i \neq k}}^{N} p^i \cdot (p^i)^T \cdot p^k - \sum_{\substack{j=1 \\ j \neq k}}^{N} p^k \cdot (p^j)^T \cdot p^k - \sum_{\substack{i=1 \\ i \neq k}}^{N} \sum_{\substack{j=1 \\ j \neq i}}^{N} p^i \cdot (p^j)^T \cdot p^k \tag{5}$$

and regrouping, we can find the coefficients for each training pattern:

$$w \cdot p^k = \underbrace{\left[(p^k)^T \cdot p^k - \sum_{\substack{j=1 \\ j \neq k}}^{N} (p^j)^T \cdot p^k \right]}_{I} \cdot p^k + \sum_{\substack{i=1 \\ i \neq k}}^{N} \underbrace{\left[\overbrace{(p^i)^T \cdot p^k}^{\text{cross talk}} - \sum_{\substack{j=1 \\ j \neq i}}^{N} (p^j)^T \cdot p^k \right]}_{I} \cdot p^i$$

(6)

Careful analysis of Equation 6 provides some insight into the behavior of the model. For this purpose, it is illustrative to first consider the response of the model when only the hebbian term in Equation 2 is included:

$$w \cdot p^k |_{\text{hebbian}} = [(p^k)^T \cdot p^k] \cdot p^k + \overbrace{\sum_{\substack{i=1 \\ i \neq k}}^{N} [(p^i)^T \cdot p^k] \cdot p^i}^{\text{cross talk}}$$

(7)

In this case, the ideal response of the model is the original pattern p^k, which corresponds to the first term in Equation 7. However, as a result of overlap with other patterns in the associative matrix $(p^i, i \neq k)$, a cross-talk term appears at the output of the system as reflected in the second term of Equation 7.

The introduction of an anti-hebbian component is aimed at reducing this cross talk while preserving the associative function of the model. In this case, we define the ideal response of the model to be an enhanced version of the original pattern p^k, one where activity in overlapping channels has been suppressed (e.g., as in Figure 3b). Two conditions must be met in order for this to occur:

$$(p^k)^T \cdot p^k > \sum_{\substack{j=1 \\ j \neq k}}^{N} (p^j)^T \cdot p^k$$

(8)

$$(p^i)^T \cdot p^k - \sum_{\substack{j=1 \\ j \neq i}}^{N} (p^j)^T \cdot p^k < 0, \quad 1 \leq i \leq N$$

(9)

Constraint 8 requires that the first term in Equation 6 be positive, thus ensuring that the correct stored pattern has the largest contribution to the output. This constraint is met when the norm of the correct pattern $(\|p^k\|)$ is larger than the sum of the projections of all other training patterns onto it.

Constraint 9 requires that the second term in Equation 6 be negative, so that not only is the cross talk eliminated, but the overlap with other patterns is also subtracted from the output. Fortunately, this second constraint is a subset of the first one. If Constraint 8 is met, it then follows that
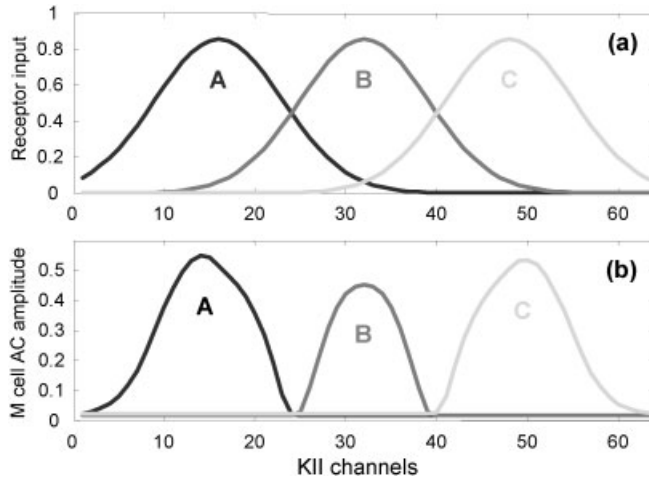
$$(p^k)^T \cdot p^k > (p^i)^T \cdot p^k$$

(10)

Figure 3. (a) Overlapping synthetic patterns used to characterize the new learning rule. (b) Output of the KIII model (i.e., AC amplitude of mitral cells), when each odor pattern is presented at the input. Note that the overlap between odor patterns at the outputs of the KIII model has been eliminated.

because the right-hand side of Equation 10 is simply one of the terms in the right-hand side of Equation 8, and patterns are assumed to be nonnegative. With this result at hand, a rearrangement of the left-hand side in Equation 9 can be used to show that the constraint is always met:

$$(p^i)^T \cdot p^k - \sum_{\substack{j=1 \\ j \neq i}}^{N} (p^j)^T \cdot p^k = \underbrace{(p^i)^T \cdot p^k - (p^k)^T \cdot p^k}_{\hat{0}} - \sum_{\substack{j=1 \\ j \neq i \\ j \neq k}}^{N} (p^j)^T \cdot p^k < 0 \qquad (11)$$

and, therefore, ensure that cross talk across patterns is entirely removed. In the following sections of this article, we empirically show that these results, obtained for a single linear step, hold true when all the dynamics of the KIII are considered.

4.2. Characterization on Synthetic Inputs

The behavior of the KIII with the new learning rule is first characterized on a synthetic data set with three classes in 64 dimensions. The input patterns are shown in Figure 3a. To facilitate visual interpretation of the results, the input channels are sorted such that activity for a particular odor pattern is localized in a specific region of the feature vector (note that a permutation of the input channels would only cause a permutation in the rows and columns of the resulting matrix w).

To better understand the role of the new hebbian/anti-hebbian rule, it is useful to isolate the connection matrices that result from each term in Equation 2. Figure 4a shows the connection matrix for the hebbian term, which is the sum of the outer product of each odor pattern with itself. As shown in the figure, the
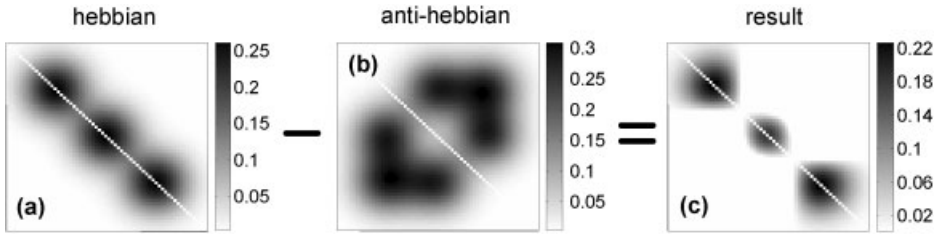
Figure 4. Lateral connections between mitral cells: (a) hebbian term, (b) anti-hebbian term, and (c) combined effect by subtracting anti-hebbian from hebbian terms.

hebbian term leads to associative connections, where input channels that are active for a given odor reinforce each other. Figure 4b shows the connectivity matrix for the anti-hebbian term, which is computed as the outer product of each odor pattern with the rest of the odor patterns. This matrix reinforces connections between channels that are active for more than one odor. By subtracting the anti-hebbian term from the hebbian term and forcing negative connections to zero, the resulting connectivity matrix (Figure 4c) is able to depress incoming/outgoing connections from/to overlapping channels. This has two important effects. First, it eliminates cross talk between patterns, as analytically predicted in the previous section. As a result, recalling one odor pattern will not elicit other stored odors. Second, the contrast between odors is significantly enhanced at the output of the KIII.

A KIII model with 64 channels was trained on the three odor patterns shown in Figure 3a using the new learning rule. Each odor pattern was then presented to the model, and the AC amplitude value of mitral activity was used as an output. Results are shown in Figure 3b. First, as predicted earlier, the recall of one odor pattern does not elicit activity in channels where other odor patterns are prevalent. Second, contrast among odor patterns is enhanced by reducing activity in channels of significant overlap.

Alternatively, one can analyze the response of individual KIII channels across odors to determine the effect of the lateral interaction on their individual receptive ranges. For this purpose, four channels with significant overlap across patterns (channels 23, 26, 38, and 41 in Figure 3) were selected and analyzed in terms of their inputs and KIII outputs for the three patterns. The results are shown in Figure 5. The inputs to the KIII model respond significantly to two of the three odor patterns. In contrast, as a result of lateral interactions, each mitral cell in the KIII model becomes specifically tuned to one odor. This result is analogous to the sharpening of the molecular receptive field first described by Mori (Yokoi et al.[19]).

5. BACKGROUND SUPPRESSION THROUGH CONTRAST ENHANCEMENT AND HABITUATION

Habituation is a process that allows a sensory system to reduce its sensitivity to previously detected stimuli, preventing sensory overflow in the central nervous
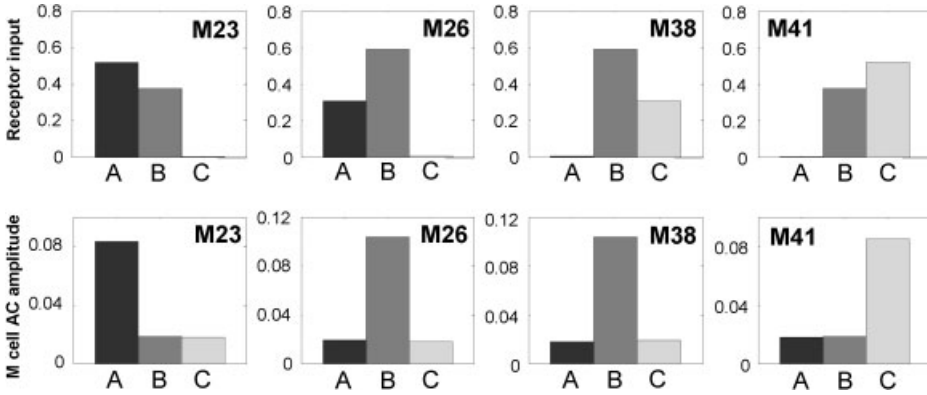
Figure 5. Activity of four KIII channels (23, 26, 38, and 41) for the three synthetic odors patterns (A, B, and C). Upper row: Input to the KIII. Lower row: AC amplitude of mitral cells.

system and improving the ability to detect new and, therefore, more informative stimuli.[22] This process has also been shown to take place in the olfactory bulb, where the response to a constant odor stimulus decreases over time.[23] In Ref. 9 we have proposed a model for odor suppression in gas sensor arrays through local habituation of KIII channels. In that earlier model, a statistical preprocessing stage was used to orthogonalize odor patterns, thus facilitating the segmentation process. In the present article, the preprocessing stage is replaced by a hebbian/ anti-hebbian recurrent circuit that, as shown in the previous sections, is able to significantly reduce the overlap across odor patterns.

Following Kozma and Freeman,[3] we assume that the habituation process induces depression of the synapses from mitral nodes onto other neuron populations (i.e., mitral to granule connections, and lateral connections between mitral cells). Changes in these synapses are assumed to be proportional to their instantaneous value and, thus, follow an exponential decay[22]:

$$\Delta w = w(t + \Delta t) - w(t) = [B - w(t)][1 - \exp(-\Delta t/\tau)] \qquad (12)$$

where w represents a synapse from the habituating mitral cell to other mitral or granule cells, τ is a time constant governing the rate of habituation, and B is the final value that the connection will approach asymptotically. Habituation parameters B and τ are borrowed from Ref. 9.

Figure 6 shows the response of the KIII model in a simple habituation scenario using the synthetic patterns in Figure 3a. The system is initially exposed to odor pattern A for 400 ms. As a result of the habituation term, the activity in the network decays toward zero in an exponential fashion. Following habituation to odor pattern A, the system is then presented with an additive mixture of odors A and B at time $t = 400$ ms. As shown in the figure, the KIII model is able to suppress the activity in those channels that code for odor A, to where the resulting output pattern is as if only odor B were present, thus allowing the system to tune its sensitivity to the new odor in the environment.
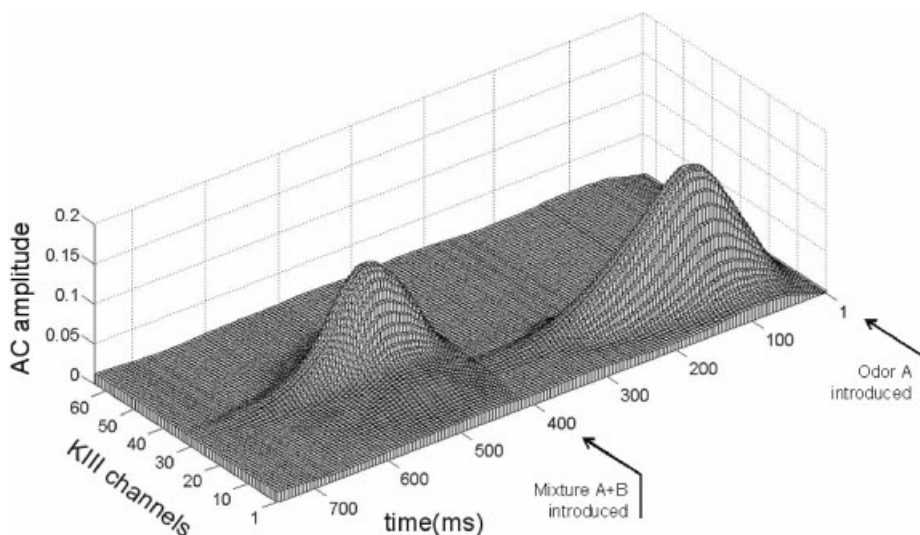
Figure 6. Evolution of the KIII mitral AC amplitude in a habituation experiment with synthetic patterns. Odor A (refer to Figure 3a) is presented to the KIII at time $t = 1$ ms, and the system is allowed to habituate. At time 400 ms, a mixture of odors A and B is introduced; the response of the system is as if only odor B was present.

6. VALIDATION ON SENSOR-ARRAY PATTERNS

The model was also validated on experimental data from a gas sensor array with four MOS sensors (TGS2600, TGS2620, TGS2611, and TGS2610).[12] The sensors were modulated in temperature[24] with a sinusoidal profile to increase the information content of the response. The sensors were exposed to the headspace of acetone (A), isopropyl alcohol (B), and ammonia (C), as well as their binary mixtures (AB, AC, and BC). The temperature-modulated response of one of the sensors was used to train the KIII model, previous L1 normalization of each response pattern. This preprocessing is necessary to balance the total input to the KIII, which ensures that the model operates in a well-behaved dynamic region.

6.1. Contrast Enhancement

The normalized sensor response patterns to the three pure analytes (A, B, and C), shown in Figure 7 (left column), were used to train the KIII model using the new learning rule. Even though the sensor provides a unique response pattern to each analyte, there is also a significant degree of overlap that shadows the most relevant discriminatory information. Figure 7 (right column) shows the output of the KIII to the three analytes; the KIII is able to noticeably reduce the overlap across patterns and enhance the channels (i.e., operating temperatures) with
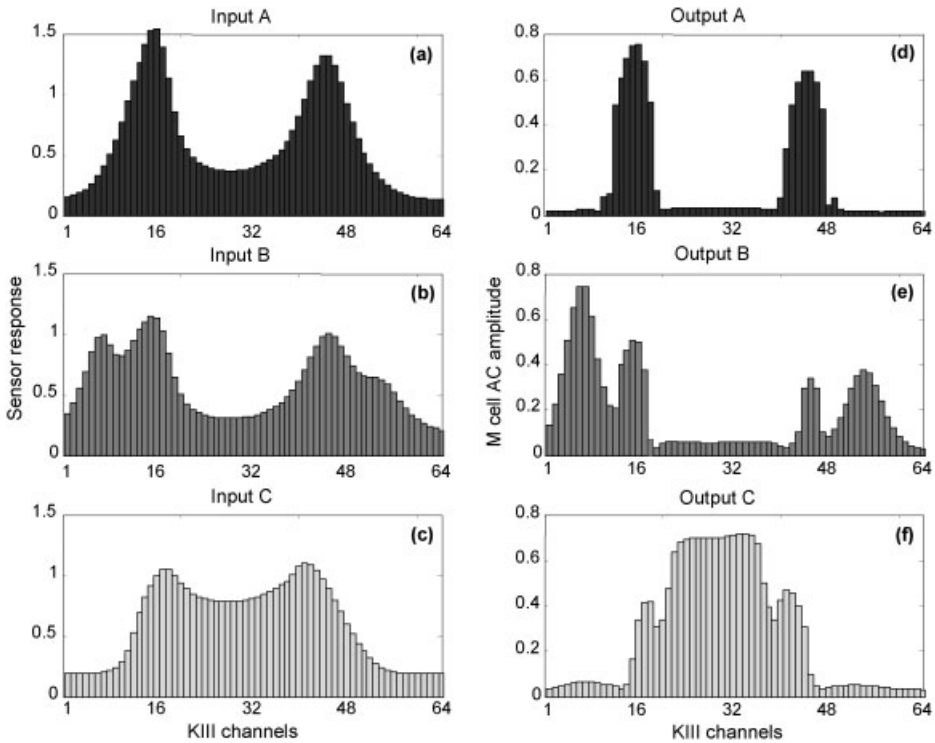
Figure 7. Contrast enhancement in the KIII with experimental data from a gas sensor. The left column shows the sensor response to the three analytes, which serves as the input to the KIII. The right column shows the corresponding output of the KIII (i.e., AC amplitude in mitral cells).

highest selectivity. The response pattern for analyte A is sharpened around the two peaks (channels 16 and 45). Although these peaks are present for the three analytes, their activity relative to other channels is highest for pattern A. A more interesting response is obtained with analyte B, for which the most discriminatory information is provided by the secondary peaks around channels 7 and 54. As a result, the trained KIII increases contrast in these channels. Note that the secondary peak around channel 53 is minimally noticeable in the original sensor response (Figure 7b), but is clearly resolved in the output of the model (Figure 7e). Finally, the sensor response pattern for analyte C is transformed by enhancing activity in the central channels, which is where discriminatory information for this analyte is highest.

The tuning range of five individual KIII channels (6, 12, 26, 38, and 52) is shown in Figure 8. These channels were chosen for temperatures that showed higher activity for each one of the three input odors. The top row shows the input to the KIII, whereas the bottom row shows the AC amplitude at the mitral outputs. We can observe that the model is able to significantly sharpen the response of
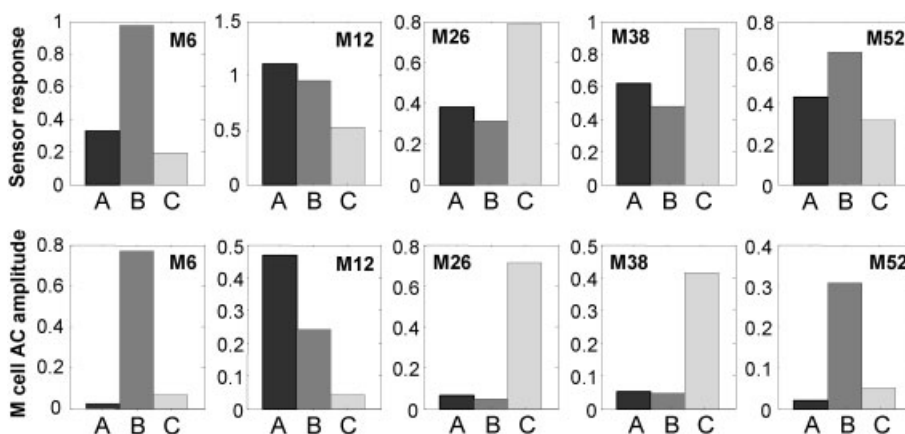
Figure 8. Activity across odors of channels 6, 12, 26, 38, and 52. Upper row: sensor response. Lower row: AC amplitude of mitral cells.

mitral nodes with respect to that in the sensor response, to where each mitral node becomes highly tuned to a particular odor. This sharpening is done in a way similar to winner-take-all competition, where only the response to the odor with highest response at the input is kept at the output.

6.2. Background Suppression

The KIII model, trained on the sensor response to the three pure compounds, was then tested on a background-suppression scenario. The system was first presented with acetone (odor A), which in this case served as a background odor, and allowed to habituate for 400 ms. At this time, the system was presented with the response pattern to a mixture of acetone (odor A) and isopropyl alcohol (odor B). Figure 9a shows the response of the KIII when trained using the new hebbian/anti-hebbian rule. Even though the two analytes are present at the input after $t = 400$ ms, the KIII shows sensitivity only to those temperatures (channels) that are specific to isopropyl alcohol (odor B). Note that the KIII response to mixture AB is not identical to the ideal response to odor B in Figure 7e but a further contrast-enhanced version (i.e., only the secondary peaks around channels 7 and 54 are active). The ability of the KIII model to respond to only one of the components in the mixture is consistent with a known olfactory perception phenomenon, know as release from mixture suppression, according to which the odor quality of a binary mixture can be shifted to one of the components by adapting to the other one.[25] To further illustrate the benefits of the new hebbian/anti-hebbian rule, Figure 9b shows the response of the KIII when trained using only the hebbian component (i.e., Equation 7). The initial stimulus elicits a response that is not unique to odor A but has characteristics from the three odors; note the presence of a secondary peak
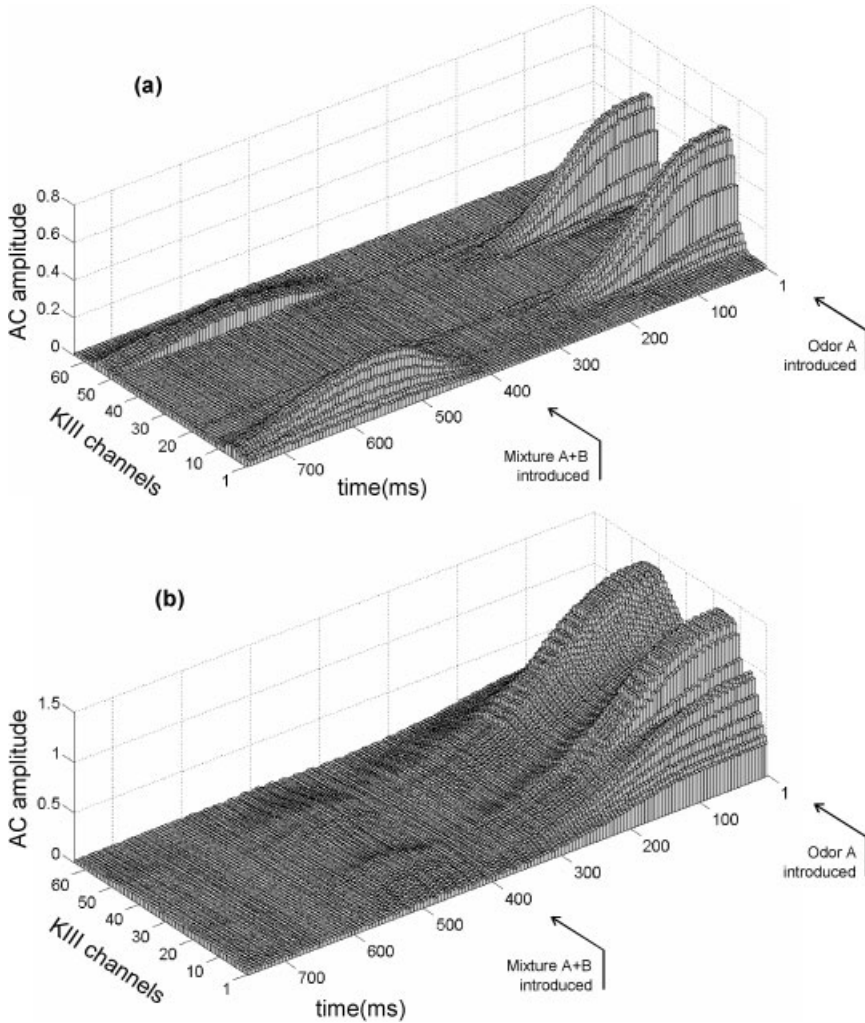
Figure 9. Habituation scenario with gas sensor response patterns. Odor A is introduced at $t = 1$ ms. Following habituation of odor A, the KIII is presented with a 50/50 mixture of odors A and B. (a) KIII model trained with the hebbian/anti-hebbian rule: The system response to mixture A + B is a contrast-enhanced version of pattern B alone. (b) KIII model trained only with the hebbian term: As a result of widespread activation, all channels habituate, and the system is unable to respond to the subsequent presentation of mixture A + B. (Time axes of both figures are mirrored to help visualize the time evolution of the channels.)

around channel 7, which is prototypical of odor B, and a high activation in the central channels, which is characteristic of odor C. This nonspecific response is due to the cross-talk term in the hebbian-only rule. As a result of widespread activation, habituation suppresses activity in all output channels, and the system is unable to respond to the subsequent presentation of mixture A + B.

7. DISCUSSION

There are two prevailing views on how odor contrast enhancement occurs at the olfactory bulb. The first, proposed by Mori and colleagues (Yokoi et al.[19] and Mori et al.[26]), states that lateral inhibitory connections sharpen the molecular receptive range (i.e., the tuning specificity) of projection neurons in the bulb, in a manner akin to edge detection through receptive fields in the retina. The second, more recent view of Laurent[27] and Laurent et al.[28] argues that contrast enhancement occurs as a global redistribution of activity across the entire olfactory bulb, as opposed to local improvements in the molecular receptive field of individual projection neurons or winner-take-all selection of the most active units. According to this view, the representation in the olfactory bulb changes continuously throughout a stimulus in an odor-specific manner; this distributed temporal patterning progressively increases the contrast between bulb-wide odor representations. From this perspective, the model proposed in this article is consistent with the view of Mori, because the main mechanism for contrast enhancement is a form of winner-take-all competition.

The proposed rule relies on a hebbian term to build associations within odors and an anti-hebbian term to reduce co-occurring activity across odors. Formal analysis on a linear neural network shows that the anti-hebbian term of the learning rule is able to completely eliminate cross talk. The learning rule has been implemented on the KIII neurodynamics model, and characterized on a synthetic data set. Our results show that the KIII is able to increase the discrimination between odors or, alternatively, sharpen the tuning specificity of individual mitral channels. In addition to performing contrast-enhancement functions, the new learning rule has also been shown to achieve odor background suppression when combined with habituation. These two computational functions have been finally validated on experimental data from a temperature-modulated sensor exposed to three analytes. The trained KIII model is able to depress activity in channels that display poor selectivity toward the analytes and increase activity in those that have more discriminatory power.

The results presented in this article provide analytical proof that, on a linear feed-forward neural network, the anti-hebbian term is able to eliminate cross talk. We argue that the anti-hebbian term has a similar effect when applied to the more complex KIII model, because the linear network represents a single step of an unfolded fully laterally connected network. Supporting this view, experimental results on the KIII show that the anti-hebbian term is able to reduce the cross talk and the overlap between patterns. However, a more throughout analysis is required to formally characterize the effect of the learning rule on the dynamic behavior of the KIII model.

Acknowledgments

References

1. Shepherd G, Greer C. Olfactory bulb. In: Shepherd G, editor. The synaptic organization of the brain. New York: Oxford University; 1979.
2. Yao Y, Freeman W. Model of biological pattern recognition with spatially chaotic dynamics. Neural Networks 1990;3:153–170.
3. Kozma R, Freeman W. Chaotic resonance-methods and applications for robust classification of noisy and variable patterns. Int J Bifurcat Chaos Appl Eng Sci 2001;11:1607–1629.
4. Chang H, Freeman W, Burke B. Local homeostasis stabilizes a model of the olfactory system globally in respect to perturbations by input during pattern classification. Int J Bifurcat Chaos Appl Eng Sci 1998;8:2107–2123.
5. Freeman W. Mass action in the nervous system: Examination of neurophysiological basis of adoptive behavior through the EEG. New York: Academic Press; 1975.
6. Clussnitzer U, Quarder S, Otto M. Interpretation of analytical patterns from the output of chaotic dynamical memories. Fresenius J Anal Chem 2001;369:698–703.
7. Quarder S, Claussnitzer U, Otto M. Using singular-value decomposition to classify spatial patterns generated by a nonlinear dynamic model of the olfactory system. Chemometr Intell Lab Syst 2001;59:45–51.
8. Otto M, Quarder S, Claußnitzer U, Lerchner J. A nonlinear dynamic system for recognizing chemicals based on chemical sensors and optical spectra. In: Proc World Multiconference on Systemics, Cybernetics and Informatics; 2000. pp 413–418.
9. Gutierrez-Osuna R, Gutierrez-Galvez A. Habituation in the KIII olfactory model with chemical sensor arrays. IEEE Trans Neural Netw 2003;14:1565–1568.
10. Persaud K, Dodd G. Analysis of discrimination mechanisms in the mammalian olfactory system using a model nose. Nature 1982;299:352–355.
11. Pearce TC, Schiffman SS, Nagle HT, Gardner JW. Handbook of machine olfaction. Weinheim: WILEY-VCH; 2003.
12. Figaro 1996. Osaka, Japan: Figaro Engineering Inc.
13. Duda R, Hart P, Stork D. Pattern classification. New York: Wiley; 2001.
14. Pearce TC. Computational parallels between the biological olfactory pathway and its analogue "The Electronic Nose": Part I. Biological olfaction. BioSystems 1997;41:43–67.
15. Pearce TC. Computational parallels between the biological olfactory pathway and its analogue "The Electronic Nose": Part II. Sensor-based machine olfaction. BioSystems 1997;41:69–90.
16. Kuzmina M, Manykin E, Surina I. Recurrent associative memory network of nonlinear coupled oscillators. In: Int Conf on Artificial Neural Networks (ICANN), Vienna, Austria; 2001. pp 433–438.
17. Kozma R, Freeman W. Encoding and recall of noisy data as chaotic spatio-temporal memory patterns in the style of the brains. In: Int Joint Conf on Neural Networks, Como, Italy; 2000. pp 52–57.
18. Principe J, personal communication; 2004.
19. Yokoi M, Mori K, Nakanishi S. Refinement of odor molecule tuning by dendrodendritic synaptic inhibition in the olfactory bulb. Proc Natl Acad Sci 1995;92:3371–3375.
20. Principe J, Euliano N, Lefebvre W. Neural and adaptive systems. New York: Wiley; 1999.
21. Haykin S. Neural networks: A comprehensive foundation. Upper Saddle River, NJ: Prentice Hall; 1999.
22. Wang D. Habituation. In: Arbib M, editor. The handbook of brain theory and neural networks. Cambridge, MA: MIT Press; 1998. pp 441–444.
23. Wilson D. Comparison of odor receptive field plasticity in the rat olfactory bulb and anterior piriform cortex. J Neurophysiol 2000;84:3036–3042.
24. Gutierrez-Osuna R, Gutierrez-Galvez A, Powar N. Transient response analysis for temperature modulated chemoresistors. Sensor Actuator B Chem 2003;93:57–66.
25. Lawless T. An olfactory analogue to release from mixture suppression in taste. Bull Psychonom Soc 1987;25:266–268.

26. Mori K, Nagao H, Yoshihara Y. The olfactory bulb: Coding and processing of odor molecule information. Science 1999;286:711–715.
27. Laurent G. Olfactory network dynamics and the coding of multidimensional signals. Nat Rev Neurosci 2002;3:884–895.
28. Laurent G, Stopfer M, Friedrich R, Ravinovich M, Volkoskii A, Abarbanel H. Odor processing as an active dynamical process: Experiments, computation and theory. Annu Rev Neurosci 2001;24:263–297.